PHYSICS AND CHEMISTRY OF SOLID STATE
V. 25, No. 4 (2024) pp. 844-852
Section: Physics

DOI: 10.15330/pcss.25.4.844-852

Vasyl Stefanyk Precarpathian National University

ФІЗИКА І ХІМІЯ ТВЕРДОГО ТІЛА
Т. 25, № 4 (2024) С. 844-852
Фізико-математичні науки

PACS: 85.60.Bt; 78.20.Bh; 73.61.Ga

ISSN 1729-4428 (Print)
ISSN 2309-8589 (Online)

R. Aliev[1], M. Komilov[1], S. Aliev[2], I. Gulomova[1]

Comparative analysis of conventional and bifaical solar cells under various illumination conditions

[1]*Andijan State University, Andijan, Uzbekistan, irodakhon.gulomov@yahoo.com*
[2]*Andijan Mechanical Engineering Institute, Andijan, Uzbekistan*

In this work, through a detailed analysis of the mechanisms of photon absorption, photogeneration processes and the efficiency of nonequilibrium charge carriers' collection under conditions of rear and double-sided illumination, the initial physical parameters of the internal layers and the design of double-sided sensitive solar cells with n^+-p junction on the front side has been studied. The modern numerical simulation method was used to study the solar cells. Models of silicon solar cells (SC) contains p^+-p-n^+ structure with separating n^+-p-junction near the frontal (upper) surface. Increasing the doping concentration in the p-region notably enhances the steepness of the I-V curve, indicative of improved quality of the solar cell and p-n junction. Specifically, an optimal doping concentration of 10^{15} cm^{-3} yields the highest efficiency, demonstrating the critical role of doping concentration in performance optimization. Furthermore, variations in doping concentration exert differential impacts on key parameters. Notably, open-circuit voltage, fill factor, efficiency, maximum output power, and serial resistivity exhibit distinct responses to changes in doping concentration. For instance, an increase in doping concentration from 10^{13} cm^{-3} to 10^{15} cm^{-3} results in notable improvements across these parameters, highlighting the significance of precise doping control in enhancing solar cell performance. When, photoelectric parameters of conventional and double side sensitive solar cells are compared, it has been found that the short circuit current and open circuit voltage of double side solar cell are 2 times and 18 mv greater than those of conventional solar cell.

Keywords: Silicon, Bifacial Solar Cell, Sentaurus TCAD, Ray Tracing, Efficiency, Fill Factor.

Received 09 March 2024; Accepted 04 November 2024.

Introduction

Photovoltaic conversion of solar energy is carried out using solar panels (SP), which are assembled from semiconductor solar cells (SC). Over the last decade, the introduction of joint ventures with double-sided-sensitive silicon solar cells has begun. SPs with double-sided sensitive silicon SCs generate significantly more energy than conventional SPs. This is due to the contribution of additional photoelectric generation of charge carriers due to diffusion solar irradiation [1, 2]. According to preliminary estimates, the advantages of double side sensitive solar cells should reach up to 25%. But, the actual additional increase in power is up to 15% [3]. In [4], it is believed that by optimizing secondary reflectors, the output power of double-sided sensitive SPs can be significantly increased. It is expected that double-side sensitive SPs will expand in the global photovoltaic market to 40% in 2025 and to 60% in 2029 [5, 6]. It is important to note that the cost of double-sided illuminated SPs is slightly higher than conventional SPs [5, 7]. An analysis of the literature indicates that the number of studies on optimization of the initial parameters and design of double-sided sensitive solar cells is insignificant. Almost two types of solar cells differ only in the design of the back electrodes. The possibilities of modern methods of texturing illuminated surfaces [8, 9] and nanoplasmonic photocurrent amplification, implemented by introducing metal nanoparticles into the bulk of a semiconductor [10, 11] to increase the efficiency of double-sided sensitive solar cells, have not been studied. More complex designs of double-sided sensitive SCs such as PERC (Passivated Emitter Rear Contact), PERT (Passivated Emitter Rear Totally Diffused) and

PERL (Passivated Emitter Rear Locally Diffused) with localized emitter layers on the back side have been developed, but the cost of such samples is significantly higher than conventional ones [12, 13]. In such solar cells with an emitter layer on the rear surface, the negative influence of a high recombination rate becomes significant [14]. There is frequent shunting *p-n*-potential-induced transitions, promoting degradation of the main photovoltaic parameters of solar cells [15, 16].

Based on the foregoing, it is advisable to assume that through a detailed analysis of the mechanisms of photon absorption, photogeneration processes and the efficiency of collection of nonequilibrium charge carriers under conditions of back and double-sided illumination, it is possible to optimize the initial physical parameters of the internal layers and the design of double-sided sensitive SCs with n^+-*p*-transition on the front side. This article is devoted to find solution the problems mentioned above.

I. Research methodology

The modern numerical simulation tool "Sentaurus TCAD" was chosen for the study. Geometric models of silicon solar cells (SCs) with the structure p^+-*p*-n^+ with separating n^+-*p* junction near the frontal (upper) surface (Fig. 1) is created in Sentaurus Structures Editor. SCs are a one-sided sensitive (Fig. 1 a) with a solid electrode on rear surface and a double-sided sensitive (Fig. 1 b, c, d) with a grid electrode on the rear and front surfaces.

To simulate the SCs using "Sentaurus TCAD", the corresponding structural and physical parameters given in table 1 were selected. Geometric models of solar cells for one-sided and double-sided illumination were created using the "Sentaurus Structure Editor" tool with code in the "Tool Command Language" (TCL). To simulate double-sided illumination of the SC, the geometric model shown in Fig. 1 was used. 2 with flat silver reflectors *00* from Aluminum. In further stages of simulation, the tools "Sentaurus Device", "Sentaurus Visual" and "Sentaurus Workbench" were used.

According to the data in Table 1 dimension of 2D solar cells in Fig. 1 and Fig. 2 are 500 microns of width and 175 microns of thickness. At the same time, the depth n^+-*p*-juntion and isotype p^+-*p*-juntion was 1 μm. Each reflector *00* in Fig. 2 oriented at an angle 45^0 to the horizon and ensures a perpendicular incidence of light on the rear surface of the solar cell after double reflection. The reflectivity of the silver reflector is assumed to be 1 to avoid the intensity loss in silver. Note that for a more detailed study of the distribution functions of light absorption, optical generation of nonequilibrium charge carriers and the process of their separation due to n^+-*p*-junction, as well as to visualize the currents of electrons and holes, the distribution of the electrostatic potential in the space charge region, the geometric model of the SC are meshed with size of 4.0 μm in X direction and 2.3 μm in Y direction. At the same time, the active regions like the n^+-*p*-junction and isotype p^+-*p*-junction, were meshed with smaller size of 0.1 μm in Y direction. Reason of the creating the mesh in geometric model is that in numerical simulation physical parameters like concentration of carriers, potential, electric field, absorbed photon density are calculate at each points. In the next section, theoretical background of numerical simulation of the solar cell using TCAD is explained in detail.

II. Theory

After creating the geometric model of the solar cells, which are suitable for one side and double side illumination, numerical simulation is carried out in two stages: optical and electrical calculation There are main three model to calculate optical properties: Transfer Matrix Method (TMM), Ray Tracing and Beam Propagation. Each model can be used to simulate solar cells, but it depends on purpose of simulation. TMM is mainly used to simulate thin layer planar solar cells. Because, it uses from electric field matrices and can consider internal interference but it cannot consider more than 1 refraction of the light. In this work, we focus on mainly double side solar cell and it is important to consider more than one refraction of the light. So the "Ray Tracing"

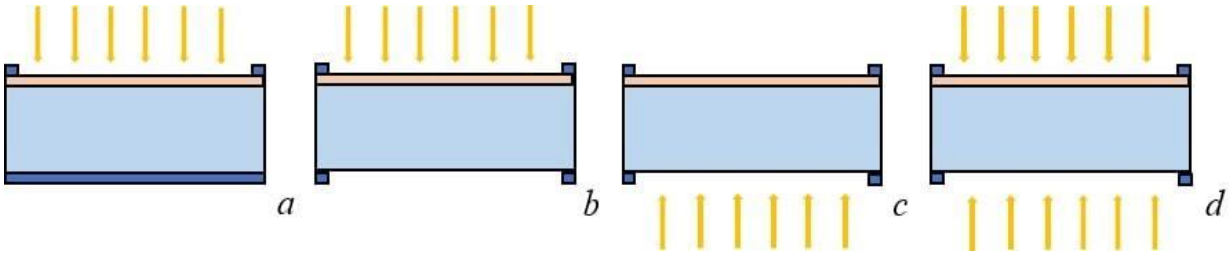

Fig. 1. Geometric models of silicon solar cells with n^+-*p*-junction with a grid electrode on the front and rear surfaces (*b, c, d*) and a solid electrode on the back surface (*a*) under frontal conditions (*a, b*), back (c) and double-sided (*d*) lighting.

Table 1.

Basic structural and physical parameters of structures

№	Layer structure and conductivity	Dopant concentration	Layer thickness	Layer width
	p^+-p-n^+	cm^{-3}	μm	μm
1	**n^+**	10^{17}	1 (0,1)	500 (4)
2	**p (base)**	10^{15}	175 (2,3)	500 (2,3)
3	**p^+**	10^{16}	1 (0,1)	500 (4)

method is chosen. In Ray tracing model, number of Rays are used as a light. Each Ray can be controlled independently and after each refracting each ray divided new to 2 independent rays which is transmitted and reflected, this is called as population. If we don't make any assumption, calculation can continue infinitely. To stop the calculation, critic power of ray is used. If power of ray is higher than critic power, calculation continue for that ray else calculation is stopped, This makes it possible to calculate, using the numerical Monte Carlo method, the processes of changing the power of the incident, reflected and transmitted ray flux under certain conditions of the accepted boundary conditions. Total power of the incident light can be written as sum of powers of absorbed, escaped and stopped rays.

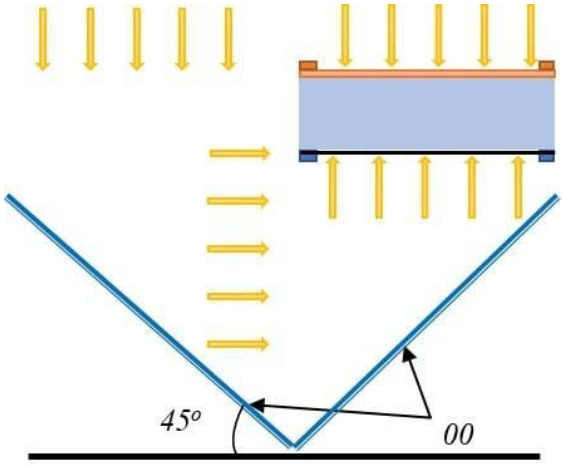

Fig. 2. Geometric model of silicon structure with n^+-p-transition with a grid electrode on the front and rear surfaces under conditions of frontal, rear and two-sided lighting (*00* – Mirror reflectors).

$$P_{total} = P_{abs} + P_{escape} + P_{stopped}\ , \qquad (1)$$

Here: P_{abs} – absorbed power; P_{escape} – power of escaped rays;$P_{stopped}$ – power of stopped rays.

When light fall on interface, it is divided to transmitted and refracted lights. To calculate relationship among angles of incident, transmitted and refracted lights, Snelli's law is used as a optical boundary condition.

$$\frac{n_1}{n_2} = \frac{sin\beta}{sin\theta}\ , \qquad (2)$$

Here: θ – angle of incident light and β– beam refraction angle.

In addition to angles, there is relationship among energies of incident, transmitted and refracted lights. In Ray Tracing, Fresnel coefficients are mainly used as energy optical boundary condition.

$$\begin{cases} r_{\perp} = \frac{n_1 \cos\alpha - n_2 \cos\gamma}{n_1 \cos\alpha + n_2 \cos\gamma} \\ t_{\perp} = \frac{2n_1 \cos\alpha}{n_1 \cos\alpha + n_2 \cos\gamma} \end{cases} \qquad (3)$$

Here: n_1 and n_2 are the refractive indices of mediums; β – the angle of incident light; γ – the angle of refracted light; r and t – the Fresnel coefficients.

The absorption of light in the medium is determined by using Burger Lambert law. By using formula 4 which is modified version of the Burger Lamber formula, optical generation can be calculated at exact point of the solar cell.:

$$G^{opt}(x, y, z, t) = I\,(x, y, z)\,[1\text{-}It\ is^{-\alpha l}]\ , \qquad (4)$$

Here: a – light absorption coefficient in the medium; l – beam path length in the sample; I – intensity of the light.

Photogenerated excitons are separated to electron and holes because of internal electric field formed in p-n junction. Carriers can move due to electric field (drift) ad difference of concentrations (diffusion). To account both of drift and diffusion transport of carriers, drift-diffusion model is used. Drift diffusion model is one of the forms of continuity equation.

$$\nabla J_n = q\left(R_{net,n} - G_{net,n}\right) + q\frac{\partial n}{\partial t} \qquad (5)$$

$$\nabla J_p = q\left(R_{net,p} - G_{net,p}\right) + q\frac{\partial p}{\partial t} \qquad (6)$$

Here: $R_{net,n}$ - and$R_{net,p}$ – recombination rates for electrons and holes;$G_{net,n}$ - and$G_{net,p}$ - generation rates for electrons and holes; J_n - and J_p – current densities for electrons and holes; n and p electron and hole concentrations; q – electron charge.

To describe the process of charge transfer in silicon, it is necessary to determine the distribution of electrostatic potential and electric field using the Poisson formula:

$$\Delta\varphi = -\frac{q}{\varepsilon}\left(p - n + N_D - N_A\right), \qquad (7)$$

Here: ε - the dielectric constant, N_D and N_A – concentration of donors and acceptors.

Calculations of the current density for electrons and holes in the studied structure taking into account the potentials in p^+-p-n^+- the structure was allowed to build their Volt-Ampere characteristics (volt-ampere characteristics). Next, based on the fundamental theory of photovoltaics, the main photovoltaic parameters of solar cells are determined.

III. Results and discussion

To identify the features of photoelectric energy conversion in double side sensitive solar cells with p^+-rn-p^+-structure, it is necessary to compare the photogeneration and charge transfer processes in them with conventional one-sided sensitive solar cells of the same structure.

Solar cells are mainly characterized by spectral and I-V characteristics. This work is devoted to comprehend physical processes in one and two sided sensitive solar cells in order to find advantages and disadvantages of both solar cells. Changing the number of illumination sides has not huge effect on spectral characteristics. So, we decided to focus on I-V characteristics of solar cells. Figure 3

shows the calculated I-V characteristics of a one-side illuminated silicon p^+-p-n^+-structures with solid rear contacts and with different doping concentrations of the p-region: *1- 10^{13}; 2- 10^{14}; 3- 10^{15} cm^{-3}*. When doping concentration of the p-region increase, the steepness of the I-V characteristics is improved. Steepness of the I-V characteristics shows quality of the solar cells and p-n junction. So, according to I-V characteristics, 10^{15} cm^{-3} is the best value of doping concentration for p-region. Change in I-V characteristics is due to effect of doping concentration on properties of materials. Besides, our optimal value of concentration agrees with other experiments [9,10].

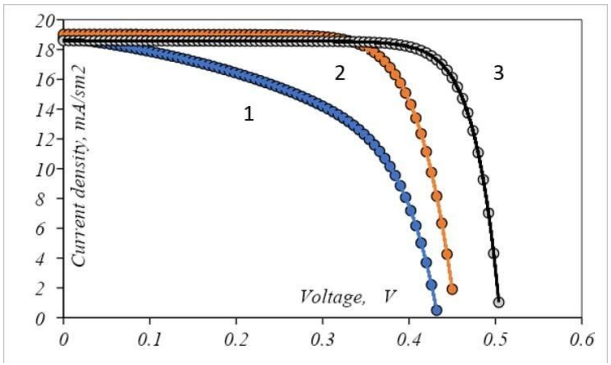

Fig. 3. I-V curves of single-snidely illuminated silicon p^+-p-p^+-structures with different base doping concentrations*p*-areas:*1- 10^{13}; 2- 10^{14}; 3- 10^{15} cm^{-3}*.

Using the data of I-V characteristics shown in Fig. 3 and based on the fundamental theory of photovoltaics, the main photovoltaic parameters of silicon solar cells given table 1 are determined. When doping concentration increase from 10^{13} cm^{-3} to 10^{15} cm^{-3}, open circuit voltage, fill factor, efficiency, maximum output power and serial resistivity are increased apart from short circuit current. Short circuit current of the solar cell with 10^{14} cm^{-3} is 19 mA/cm^2 and it is highest value among all concentrations. Increasing doping concentration of the p region increase the recombination rate and improve the conductivity at the same time. The doping concentration in the p-region influences the built-in potential across the p-n junction. This built-in potential affects the separation and movement of generated electron-hole pairs under illumination. An optimal built-in potential ensures efficient collection of photo-generated carriers without excessive recombination. Open circuit voltage is proportional to built in potential. Higher open circuit voltage means better built in potential. Therefore, silicon solar cells achieved highest efficiency of 11.8 % with 10^{15} cm^{-3} concentration.

I-V characteristics of double-sided-sensitive p^+-p-n^+-structures with different doping concentrations in p-regions:*1- 10^{13}; 2- 10^{14}; 3- 10^{15} cm^{-3}* when illuminated from the front (*a*) and back (*b*) sides are shown in Fig. 4. In condition of front side illumination, the changing of steepness of I-V characteristics depending on doping concentration of p region is similar to that of conventional one side silicon solar cell with solid rear contact. But, short circuit current decreased dramatically when doping concentration increase. Because formation of the front and rear contacts are the same in double sided sensitive solar cell so rear contact is also in grid form as front contact. If electron and holes are photogenerated in the area middle of the grid contact, possibility of recombination is higher than that solar cells with solid rear contact. In condition of rear side illumination, steepness of solar cells are almost the same but short circuit current decreased proportional to doping concentration.

To compare various illumination conditions, it is better to look at photoelectric parameters of solar cell. In table 3, photoelectric parameters of double side sensitive solar cell in condition of front and rear side illumination are given. In both conditions, when doping concentration

Table 2.

Photoelectric parameters of one-side illuminated p^+- n-p^+ structures with a rear contact

N_p (cm^{-3})	IN_{oc} (V)	J_{sc}(mA/cm^2)	FF	EFF (%)	P_{mpp} (IN)	R_s (Ohm)
10^{13}	0.438	18.85	0.534	6.97	4.41	1.427
10^{14}	0.456	19.00	0.740	10.13	6.41	3.123
10^{15}	0.510	18.58	0.788	11.80	7.47	3.157

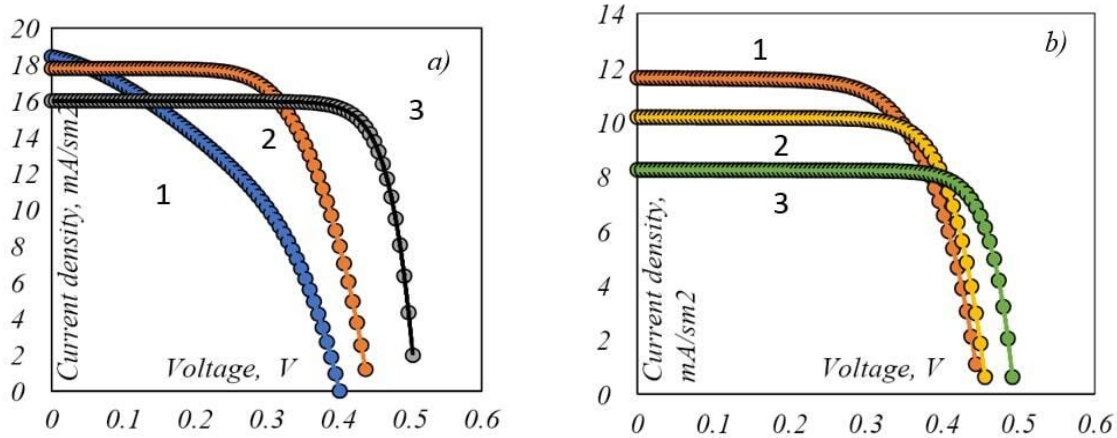

Fig. 4. I-V curves of double-sided-sensitive silicon p$^+$-p-p$^+$-structures with different base doping concentrations p-areas: 1- 10^{13}; 2- 10^{14}; 3- 10^{15} cm^{-3} when illuminated from the front (a) and back (V) sides(base thickness 2.5 microns, width 4 microns).

increase, open circuit voltage and fill factor increase and short circuit current decrease almost linearly. But efficiency in rear side illumination is decreased. Because, when solar cell illuminated from rear side, photons are absorbed mainly in rear side far from p-n junction. Higher doping concentration means higher recombination rate. In 10^{13} and 10^{14} doping concentration, short circuit currents of one side sensitive and front side illuminated double side sensitive solar cells are almost the same. But, there is 2 mA/cm^2 difference in 10^{15} cm^{-3} concentration. It is because of higher recombination rate and grid form of the rear contact. Carriers should pass longer path to reach rear contact in double sided sesitive solar cell than conventional solar cell with solid rear contact. Fill factor is parameter which shows steepness of I-V characteristics. That's why, it increase depending on concentration.

In condition of both side illumination, I-V characteristics of double side sensitive solar cell with different doping concentrations of the p region: *1- 10^{13}; 2- 10^{14}; 3- 10^{15} cm^{-3}* are shown in Fig. 5. Steepness of I-V characteristics of double side sensitive solar cell with 10^{13} cm^{-3} and 10^{14} cm^{-3} concentration of p region is more improved that that of I-V characteristics calculated for front side illumination condition of double side sensitive solar cell and for conventional solar cell with solid rear contact. Quality of the I-V characteristics for both side illumination can be considered that is avarage quality of the I-V characteristics of only front and rear side illumination conditions.

In table 4, photoelectric parameters of double side sensitive solar cell for both side illumination condition is given. Changing of the photoelectric parameters depending on doping concentration is almost the same with only front side illumination condition. It means that front side illumination contribution is higher than rear side illumination. Because, p-n junction is near to front side of solar cell.

In case of both side illumination, maximum value of short circuit current of double side sensitive solar cell is 27.5 mA/cm^2 in 10^{13} cm^3 doping concentration, voltage is 0.53 V, output power is 11.33 mW/cm^2 and efficiency is 17.91% in 10^{15} cm^3 doping concentration.

The calculated data given in table. 2 – 4 are summarized in the form of diagrams shown in Fig. 6. Figure 6 shows the short circuit current, open circuit voltage (A), power and fill factor (B) of conventional solar cell with solid rear contact and double side sensitive solar cell with various concentration of p-region in front, rear and both side illumination conditions. Double side sensitive solar cell with 10^{13} cm^{-3} doping concentration of p region in both side illumination is achieved maximum short circuit current of 33 mA/cm^2. For all solar cells in all illumination conditions, open circuit voltage is increased when doping concentration increase. Maximum open

Table 3.

Photoelectric parameters of double side sensitive solar cell in conditions of front and rear side illuminations

	N_p (sm^{-3})	IN_{oc} (IN)	J_{sc}(mA/cm^2)	FF	EFF (%)	P_{mpp} (wt)	R_s (Oh)
Front	10^{13}	0.438	11.13	0.503	3.88	2.45	1.242
	10^{14}	0.456	11.03	0.723	5.75	3.64	5.758
	10^{15}	0.504	10.91	0.788	6.88	4.33	5.510
Rear	10^{13}	0.450	11.63	0.662	5.47	3.46	6.138
	10^{14}	0.462	10.17	0.737	5.47	3.46	6.751
	10^{15}	0.498	8.24	0.785	5.09	3.22	5.713

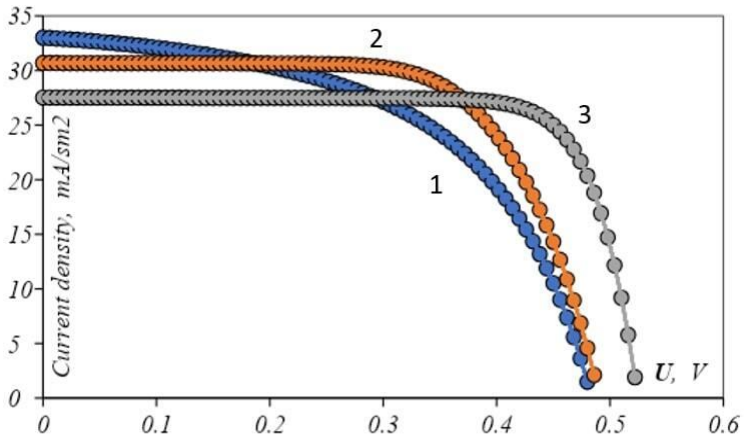

Fig. 5. I-V characteristics of double-sided illuminated silicon *solar cell* with different doping concentrations of the p region:*1- 10^{13}; 2- 10^{14}; 3- 10^{15} cm^{-3}* in both side illumination condition.

Table 4.

Photoelectric parameters of double side sensitive solar cell in both side illumination condition

N_p (sm^{-3})	IN_{oc} (IN)	J_{sc}(mA/cm^2)	FF	EFF (%)	P_{mpp} (wt)	R_s (Oh)
10^{13}	0.486	33.00	0.528	6,7	8.48	0.441
10^{14}	0.492	30.68	0.671	8,0	10.13	2.818
10^{15}	0.528	27.52	0.780	8,9	11.33	2.268

circuit voltage of 0.528 V is observed for double side sensitive solar cell with 10^{15} cm^{-3} doping concentration of p region in both side illumination.

Figure 6B and 6C shows that when both side of double side sensitive solar cells is illuminated, the efficiency decrease from 11.8% to 8.9% but output power increase from 7.47 W to 11.33 W.

It would be of interest to compare the photoelectric parameters of double side sensitive solar cell in both side illumination and conventional solar cell. According to Figure 6.a, it is found that short circuit current of double side sensitive solar cell with both side illumination is almost two times greater than that of conventional solar cell. Because, both side of double side sensitive solar cell are illuminated with the same intensity. It means that double side solar cell absorbs two times more photons than conventional solar cells. In figure 7, abosorbed photon concentration distribution of double side sensitive and conventional solar cells under various illumination conditions are shown. Maximum absorbed photon concentration is 1.77e21 for conventional solar cell and 2.38e21 for double side sensitive solar cell. Because, in double side sensitive solar cells, light falling on front side has contribution to absorbed photons in rear side in addition to light falling on rear side and the same for absorbed photon concentration in front side. Besides, concentration of absorbed photons is high in both side of double side sensitive solar cell and it is high only in front

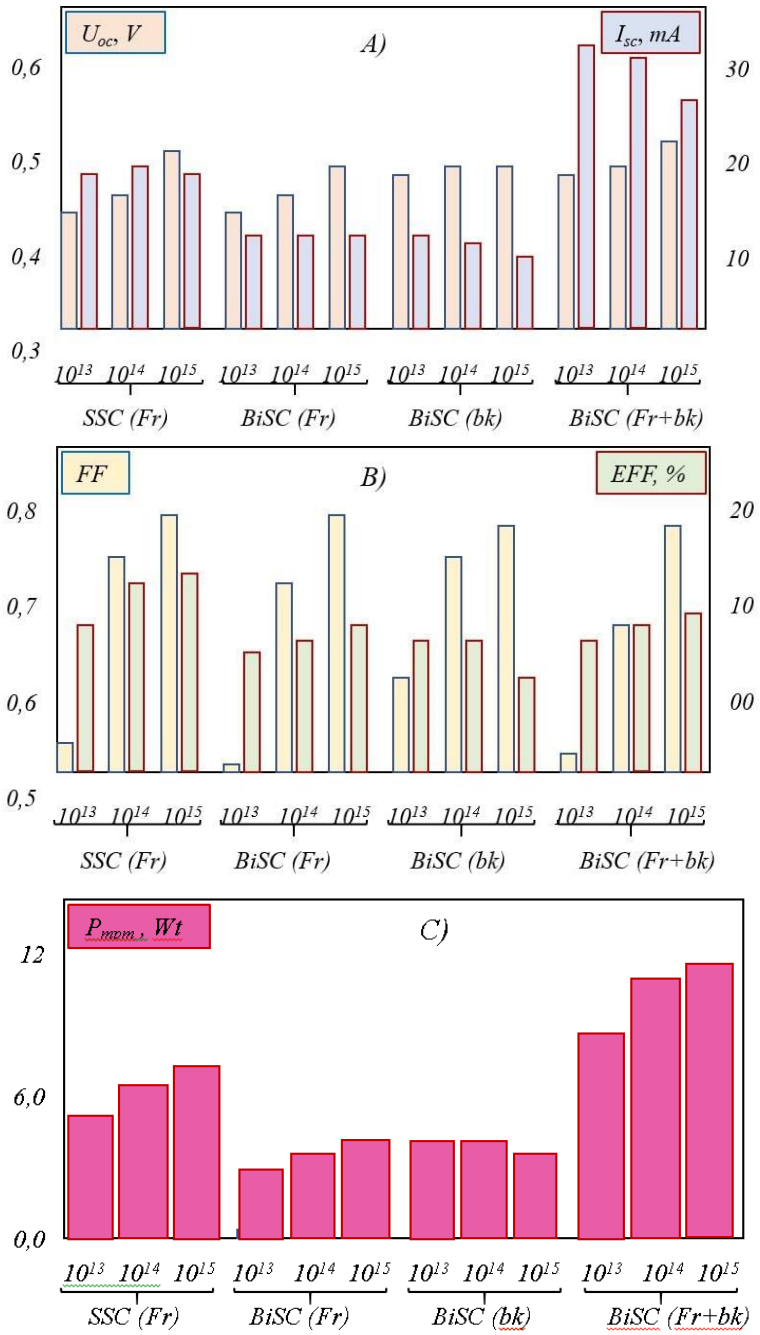

Fig. 6. Diagram $U_{oc}(N_A)$ and $I_{sc}(N_A)$ *(A) and* $FF(N_A)$ and $EFF(N_A)$ (B) and $P_{mpm}(N_A)$ *(C)* conventional and double-sided sensitive solar cells for illumination conditions: *SSC (Fr)* – conventional solar cell illuminated from the front; BiSC (Fr) – double-sided solar cell illuminated from the front; BiSC (bk) - double-sided SC illuminated from the rear; BiSC (Fr+bk) - double-sided SC illuminated from the front and rear.

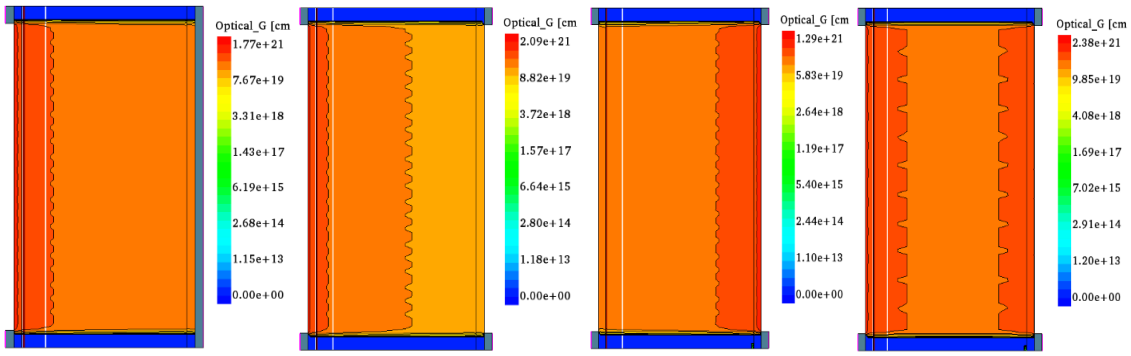

Fig. 7. Distribution of photo-generation level in conventional *(a)* and double side sensitive*(b, c, d)* SC when illuminated from the front*(b)*, rear*(c)* and both sides*(d)*.

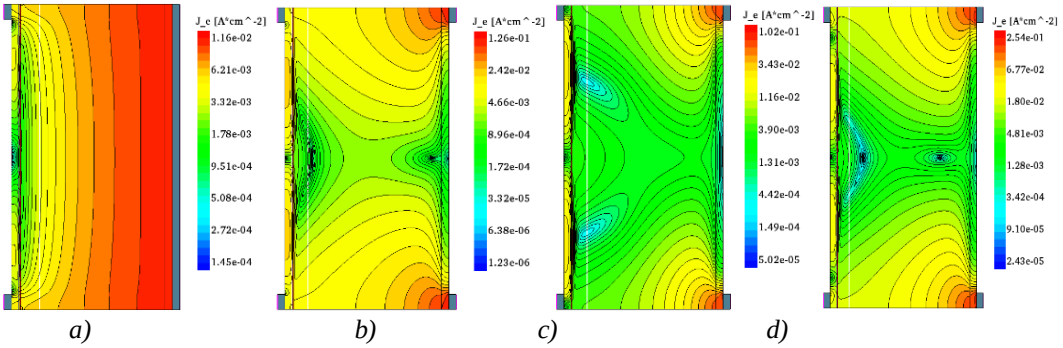

Fig. 8. Distribution of current density in a conventional*(a)* and double side sensitive*(b, c, d)* SC when illuminated from the front*(b)*, rear*(c)* both sides*(d)*.

side for conventional solar cell. So, overall absorbed photon concentration of double side sensitive solar cell is higher than that of conventional solar cell. Short circuit current is proportional to absorbed photon concentration. Based on the patterns of optical generation of nonequilibrium charge carriers in the bulk of silicon p^+-p-p^+-structures in different lighting conditions shown in Fig. 7 we can notice the following distribution of the generation level of nonequilibrium charge carriers in the volume of a conventional SC *(a)* characterized by three sections in depth: 1) the highest level of generation in the emitter p^+-layer; 2) average generation level in the space charge region p^+-n-junction; 3) more uniform generation level in the area p-region. In the case of frontal illumination of a double-sided sensitive SC *(b)*, a different distribution of the level of generation of nonequilibrium charge carriers is observed.. The base region of the silicon solar cell is divided into two sections with different generation levels. In the case of rear side illumination of a double-sided sensitive SC*(c)*, similar with conventional SC is observed *(a)* distribution of the generation level of nonequilibrium charge carriers. In the case of both side illumination of a double-sided sensitive SC*(d)*, There is a generation level symmetrical on both sides with a significantly high (almost 2.5 times) value on the rear side.

Dependences of short circuit current of conventional and double side sensitive solar cell on doping concentration in p region are different. When doping concentration increase, the recombination rate also increases and conductivity improves. Because, each doping atoms create energy trap in band gap of the silicon and it works as recombination center. So, in conventional and double side sensitive solar cells, possibility of reaching the photogenerated carriers to contacts are different. In figure 8, distribution of the current density of conventional and double side sensitive solar cells under various illumination conditions are shown. In conventional solar cells, current density is high in area near to rear contact and the same along X direction. In double side sensitive solar cells, current density is high only areas near to contacts. In middle of the two contacts, there is area with very low current density. It means that photogenerated all electrons and holes in that area cannot reach to the contacts because they should travel more path to reach contacts than in case of conventional solar cell. That's why, short circuit current of double side sensitive solar cell under front side illumination is lower than that of conventional solar cell for 10^{15} cm^{-3} concentration but the same for 10^{13} cm^{-3} and 10^{14} cm^{-3} concentrations.

Conclusion

Thus, in this work, we analyzed the influence of the doping level of the base region of the silicon p^+-p-p^+-structures on the main photovoltaic parameters in different illumination conditions, front and back surfaces separately and on both sides. As a method for simulation of silicon n^+-p-p^+ -structures the "Sentauruse TCAD" tool has been used. In order to compare with experimental data, the size of geometric model of silicon n^+-p-p^+-structures are chosen close to real industrial solar cells.

The obtained calculation results allowed us to formulate the following main conclusions:

- For single-sided illuminated solar cells, it is advisable to make the back electrode in the form of a solid layer of metal than the grid form, which is associated with the reflection of solar radiation passing through the silicon from it, which promotes more efficient absorption in the volume of silicon, stimulating greater photogeneration of current and voltage;

- With both side illumination of double side sensitive solar cells from the front and rear sides, the magnitude of the total short-circuit current, open circuit voltage and the effective power of the studied structure increases, respectively, by 53%, 3.5% and 52% than in the case of lighting from the front side, which confirms the feasibility of introducing double side sensitive solar cells;

- It is advisable to conduct further research to clarify the influence of texturing of both surfaces and the effect of nanoplasmonics on photoelectric efficiency bilaterally sensitive SCs.

In our future works, we will study different pattern of the front and rear contacts. Because, in this work, we found that pattern of contacts can influence significantly on photoelectric parameters of double sided sensitive solar cell.

Aliev R. – Head of Renewable Energy Source Laboratory, Doctor of Technical Sciences, Professor;
Komilov M. – PhD doctoral student at Andijan State University;
Aliev S. – Vice rector of Andijan Mechanical Engineering Institute, Dr. Phys.-Math. Sciences (PhD) ;
Gulomova I. – PhD Student at Andijan State University.

[1] D. Kurz, K. Lewandowski, M. Szydłowska, *Analysis of efficiency of photovoltaic bifacial cells*. In Proceedings of the ITM Web of Conferences 19/2018, Pozna´n, Poland, 01020 (2018); https://doi.org/10.1051/itmconf/20181901020.

[2] T. Aoyama, M. Aoki, I. Sumita, Z. Yoshino, A. Ogura, *Effect of Glass Frit in Metallization Paste on the Electrical Losses in Bifacial N-type Crystalline Silicon Solar Cells.* In Proceedings of the 43rd IEEE Photovoltaic Specialists Conference (PVSC), Portland, OR, USA, 2854 (2016); https://doi.org/10.1109/PVSC.2016.7750175.

[3] A. Schmid, C. Reise, *Realistic Yield Expectations for Bifacial PV Systems—An Assessment of Announced, Predicted and Observed Benefits*, Fraunhofer Institute for Solar Energy Systems ISE, 2015, Kolonia. Url: https://www.tuv.com/media/corporate /solar1/pvmodulworkshop2/42ReiseRealisticYield_Expectations_for_Bifacial_PV_Systems.pdf

[4] H. Langels, F. Gannedahl, *BiFacial PV Systems A Technological and Financial Comparison between BiFacial and Standard PV Panels*, Uppsala, 2018. Available online: https://www.diva-portal.org/smash/get/diva2:1218780/FULLTEXT01.pdf

[5] International Technology Roadmap for PV(ITRPV) 2018 Results, Version 10. Available online: https://itrpv.vdma.org/en/

[6] X. Wang, A. Barnett, *The Evolving Value of Photovoltaic Module Efficiency*, Appl. Sci., 9, 1227 (2019); https://doi.org/10.3390/app9061227.

[7] G.J. Faturrochman, M.M. de Jong; R. Santbergen, W. Folkerts, M. Zeman, A.H.M. Smets, *Maximising annual yield of bifacial photovoltaic noise barriers*, Sol. Energy, 162, 300 (2018); https://doi.org/10.1016/j.solener.2018.01.001.

[8] J. Gulomov, R. Aliev. *Influence of the Angle of Incident Light on the Performance of Textured Silicon Solar Cells*, Journal of Nano- and Electronic Physics, Volume 13(6), 060361 (2021); https://doi.org/10.21272/jnep.13(6).06036.

[9] J. Gulomov, R. Aliev. *Analyzing periodical textured silicon solar cells by the TCAD modeling*, Information technologies mechanics and optics, 21(5), 626 (2021); https://doi.org/10.17586/2226-1494-2021-21-5-626-632.

[10] J. Gulomov, R. Aliev. *Study of the Temperature Coefficient of the Main Photoelectric Parameters of Silicon Solar Cells with Various Nanoparticles*, Journal of Nano- and Electronic Physics, 13(4), 040331 (2021); https://doi.org/10.21272/jnep.13(4).04033.

[11] J. Gulomov, R. Aliev. *Numerical analysis of the effect of illumination intensity on photoelectric parameters of the silicon solar cell with various metal nanoparticles*, Nanosystems: physics, chemistry, mathematics, 12(5), 569 (2021); https://doi.org/10.17586/2220-8054-2021-12-5-569-574.

[12] Caixia Zhang, Honglie Shen, Luanhong Sun et al. *Bifacial p-Type PERC Solar Cell with Efficiency over 22% Using Laser Doped Selective Emitter*, Energies, 13, 1388 (2020); https://doi.org/10.3390/en13061388.

[13] Jinyoun Cho, Hae-Na-Ra Shin, Jieun Lee et al. *21%-Efficient n-type rear-junction PERT solar cell with industrial thin 156mm Cz single crystalline silicon wafer*, 5th International Conference on Silicon Photovoltaics, SiliconPV. 2015, Energy Procedia, 77, 279 (2015); https://doi.org/10.1016/j.egypro.2015.07.039.

[14] W. Luo, et al., *Potential-induced degradation in photovoltaic modules: a critical review*, Energy Environ. Sci., 10(1), 43 (2017).

[15] J. Bauer, V. Naumann, S. Großer et al. *On the mechanism of potential-induced degradation in crystalline silicon solar cells*, Phys. Status Solidi Rapid Res. Lett., 6(8), 331(2012); https://doi.org/10.1002/pssr.201206276.

[16] V. Naumann, O. Breitenstein, J. Bauer, C. Hagendorf, *Search for microstructural defects as nuclei for PID-shunts in silicon solar cells*, 2017 IEEE 44th Photovoltaic Specialist Conference, PVSC), 1376 (2017); https://doi.org/10.1109/PVSC.2017.8366322.

Р. Алієв, М. Комілов[1], С. Алієв[2], І. Гуломова[1]

Порівняльний аналіз звичайних і двофазних сонячних елементів за різних умов освітлення

[1]*Андижанський державний університет, Андижан, Узбекистан, irodakhon.gulomov@yahoo.com*
[2] *Андижанський машинобудівний інститут, Андижан, Узбекистан*

У роботі шляхом детального аналізу механізмів поглинання фотонів, процесів фотогенерації та ефективності збору нерівноважних носіїв заряду в умовах тильного та двостороннього освітлення визначено вихідні фізичні параметри внутрішніх шарів, а також конструкцію двостороннього освітлення. Досліджено односторонні чутливі сонячні елементи з n+-p-переходом на лицьовій стороні. Для дослідження сонячних елементів використано сучасний метод чисельного моделювання. Моделі кремнієвих сонячних елементів (СК) містять p+-p-n+ структуру із роздільним n+-p-переходом біля фронтальної (верхньої) поверхні. Збільшення концентрації легування в p-області помітно збільшує крутизну ВАХ, що вказує на покращену якість сонячного елемента та p-n-переходу. Зокрема, найвищу ефективність дає оптимальна концентрація легування 10^{15} см$^{-3}$, демонструючи критичну роль концентрації легування при оптимізації продуктивності. Крім того, коливання концентрації легуючої домішки диференційовано впливають на ключові параметри. Примітно, що напруга холостого ходу, коефіцієнт заповнення, ККД, максимальна вихідна потужність і послідовний питомий опір демонструють чітку реакцію на зміни концентрації легованої компоненти. Наприклад, збільшення концентрації з 10^{13} см$^{-3}$ до 10^{15} см$^{-3}$ призводить до помітних покращень цих параметрів, підкреслюючи важливість точного допінг-контролю для підвищення продуктивності сонячних елементів. Під час порівняння фотоелектричних параметрів звичайних і двосторонніх чутливих сонячних елементів було виявлено, що струм короткого замикання та напруга холостого ходу двосторонніх сонячних елементів у 2 рази та на 18 мВ більші, ніж у звичайних сонячних елементів.

Ключові слова: кремній, двосторонній сонячний елемент, Sentaurus TCAD, трасування променів, ефективність, коефіцієнт заповнення.